Long-Term Drift Measurements in MEMS-Based Mass Flow Controllers

Elizabeth Lawrence and Albert K. Henning

Redwood Microsystems, Inc., 959 Hamilton Avenue, Menlo Park, CA 94025

ABSTRACT

Micro-electromechanical systems (MEMS) components find increasing use in devices which measure and control gas flow, for medical and industrial use. Little or no information on the reliability of these devices has been published. This work reports the results of long-term performance studies of pressure-based mass flow controllers (MFCs) comprised of MEMS microvalves, pressure sensors, and critical flow orifices. Specifically, the details of long-term drift in the silicon pressure sensors (which comprise the flow sensor) are presented. Generally, pressure-based MFCs using MEMS components retain a flow accuracy of better than 1% of full scale over a 20:1 dynamic range, with response time under 0.5 sec, after more than three million operation cycles. The primary cause of inaccuracy within this dynamic range, and of inaccuracy larger than 1% of full scale beyond this range, is attributable to uncompensated zero-offset drift in the silicon pressure sensors, whose behavior is intrinsic to the flow sensor. Data is presented which details this characteristic, across many MFCs. Mechanical, thermal, fluidic, pneumatic and electronic mechanisms possibly responsible for the drift are also presented. Means to overcome this long-term drift phenomenon in silicon pressure sensors will complete the discussion.

Keywords: MEMS, microvalve, microfluidics, mass flow control, pressure sensor, flow sensor, reliability

1. INTRODUCTION

MEMS-based components used to control the flow and distribution of gases, for a variety of applications, have been reported in the research literature for some time. For instance, the literature on microvalves is quite extensive.[1] Many actuation methods for microvalves have been reported, including pneumatic, thermopneumatic[2], piezoelectric[3], bimetallic[4], shape-memory-alloy (SMA)[5], and electrostatic[6]. Flow sensors have also received a great deal of attention. Most sensors have focused on so-called thermal flow sensing, where a heat pulse is launched in the upstream portion of a flow field, and the time constant for the pulse to reach a downstream sensor is calibrated to the actual flow[7-9]. Alternative thermal flow sensors use the pyroelectric effect[10]. Pressure-based flow sensing has a long history in the literature of fluid mechanics. Its application using MEMS components, however, is a relatively recent phenomenon[11-14].

A flow sensor, when combined with a microvalve, and including means to command the microvalve to open or close, so as to equilibrate the flow sensor flow with a commanded flow, comprises a mass flow controller[15-17]. When the flow sensor is a pressure-based flow sensor, then the MFC is called a pressure-based MFC. These devices have been shown to deliver the highest reported accuracy for MFCs, over a wide dynamic range, with a full-scale response time (~ 100-250 msec) acceptable for most applications. Full-scale flow rates are between 1 and 1000 sccm (nitrogen equivalent), with work underway to extend the range to higher flows. The dynamic range is up to 20:1 within these full-scale flow ranges and response times, with accuracy better than 1% of reading. For the thermopneumatically-actuated microvalves used in these MFCs, it is possible to trade-off response time against dynamic range. For instance, a dynamic range of 80:1 is achieved, if the response time is relaxed to 0.8-1.0 sec. The limitation in these specifications is primarily due to the use of piezoresistive pressure sensors, which is the primary focus of this work.

2. SENSOR CALIBRATIONS AND FLOW MODEL

Figure 1 shows a detailed component schematic of the pressure-based MFCs used in this work. The thermopneumatically-actuated microvalve is seen in the upper left. The flow sensor is comprised of three functional parts: a micromachined silicon orifice, with diameter typically between 40 μm and 400 μm; an integrated-circuit temperature sensor; and, two piezoresistive pressure sensors[18-22]. The flow through the orifice can be sonic or subsonic, depending upon the pressure boundary conditions as measured by the pressure sensors. The pressure sensors are depicted functionally in Figure 2. The piezoresistors are located near the edges of a thin silicon membrane. The membrane deforms in response to a differential

pressure on either side of the sensor. The peak stress occurs near the midpoint of the sides of the membrane. Diffused silicon resistors located at these points thus can manifest the maximum change in resistance, as they respond piezoelectrically to changes in material stress. If the resistors are arranged so that one pair exhibits maximum change with respect to deformation, while the other pair exhibits minimum change, then the resistors can be arrayed in the Wheatstone bridge configuration shown. The sensor then delivers a voltage output, which is proportional to the pressure difference across the sensor membrane. For use in the pressure-based MFC, the pressure on one side of each sensor is fixed to a vacuum reference, through the use of a sealed cavity as part of the MFC package. Once installed, the pressure sensors are calibrated using a NIST-traceable standard, which leaves the sensors as measures of absolute pressure on either side of the orifice in the flow sensor. This calibration is performed as a function of temperature and pressure, since each sensor has a unique offset voltage at zero pressure differential, and a unique 'span' (slope of output voltage vs. pressure), and a unique temperature dependence of offset and span. Figure 3a shows the output voltage of the sensor as a function of pressure, while Figure 3b shows the temperature dependence of the output, for a typical pressure sensor.

Flow in the flow sensor is then calibrated by comparing the absolute pressures (derived from the pressure sensors using the above-described pressure calibration process) on either side of the orifice, against the independently-measured flow. Independent flow measurement is accomplished in steady-state, using a NIST-traceable DH Molbloc/Molbox system (DH Instruments, Phoenix, AZ). The calibration information is stored in memory, as part of the electronic circuitry which provides feedback control utilizing the flow sensor, the flow setpoint from the user, and the microvalve.

The details of the flow model, coupling the pressure sensor output to the actual flow, have been reported elsewhere[23], and are summarized here for completeness. Figure 4 shows the control schematic for the pressure-based MFC. In the figure, the critical orifice (CO) and the pressure sensors P_x and P_{out} comprise the flow sensor. The equations which govern the flow through either the microvalve or the orifice are as follows:

$$\dot{m}_{sonic} = C_d A_{eff} \frac{P_x}{\sqrt{RT}} \sqrt{\gamma \left(\frac{2}{1+\gamma} \right)^{\frac{\gamma+1}{\gamma-1}}}$$

$$\dot{m}_{subsonic} = C_d A_{eff} \frac{P_x}{\sqrt{RT}} \left(\frac{2\gamma}{\gamma-1} \right)^{1/2} \left(\frac{P_{out}}{P_x} \right)^{\frac{\gamma+1}{2\gamma}} \sqrt{\left(\frac{P_x}{P_{out}} \right)^{\frac{\gamma-1}{\gamma}} - 1}$$

$$A_{eff,CO} = D^2_{orifice}$$

$$\sqrt{A_{eff,valve}} = D \left\{ 1 - \exp\left[-\frac{z/D}{(z/D)_0} \right] \right\}$$

For the CO, the effective area A_{eff} is simply the orifice cross-sectional area. For the normally-open (NO) valve, the effective area is given by the exponential function shown, which accounts for the effect of the membrane-to-valve-seat gap z as it becomes small. Figure 4 shows schematically the arrangement of the various components in the MFC, including the flow sensor and the microvalve, the nomenclature for the nodal pressures, and the qualitative positioning of the flow control electronics, and pressure and flow calibrations, in the overall MFC control scheme.

The uncertainty of the flow can be related to variations in the structural parameters and boundary conditions (pressure and temperature) found in the flow equations. For all intents and purposes, the variations in the pressure sensors contribute the greatest uncertainty in the determination of flow. For the pressure sensors used in pressure-based MFCs, the uncertainty relations of interest is:

$$U_{\dot{m}} = \sqrt{\left(\frac{d\dot{m}}{dP_x}U_{P_x}\right)^2 + \left(\frac{d\dot{m}}{dP_{out}}U_{P_{out}}\right)^2}$$

$$\Rightarrow \frac{U_{\dot{m},sonic}}{\dot{m}_{sonic}} = \frac{U_{P_x}}{P_x}$$

$$\Rightarrow \frac{U_{\dot{m},subsonic}}{\dot{m}_{subsonic}} = \sqrt{\left(\frac{U_{P_x}}{P_x}\left\{1-\frac{\gamma+1}{2\gamma}+\frac{1}{2}\frac{\gamma-1}{\gamma}\left(\frac{P_x}{P_{out}}\right)^{\frac{\gamma-1}{\gamma}}\frac{1}{\left(\frac{P_x}{P_{out}}\right)^{\frac{\gamma-1}{\gamma}}-1}\right\}\right)^2 + \left(\frac{U_{P_{out}}}{P_{out}}\left\{\frac{\gamma+1}{2\gamma}-\frac{1}{2}\frac{\gamma-1}{\gamma}\left(\frac{P_x}{P_{out}}\right)^{\frac{\gamma-1}{\gamma}}\frac{1}{\left(\frac{P_x}{P_{out}}\right)^{\frac{\gamma-1}{\gamma}}-1}\right\}\right)^2}$$

As can be seen from these expressions, when the flow sensor flow is sonic, only the upstream pressure is required to determine the flow, and the uncertainty is greatly improved (made smaller). For the MFCs in this study, a typical flow uncertainty over a 20:1 dynamic range is about 0.25% of reading at the low end of the dynamic range. This low end corresponds to an inlet pressure of the flow sensor of about 40 Torr (see Figure 5). Sonic flow will be the focus for the remainder of the work here.

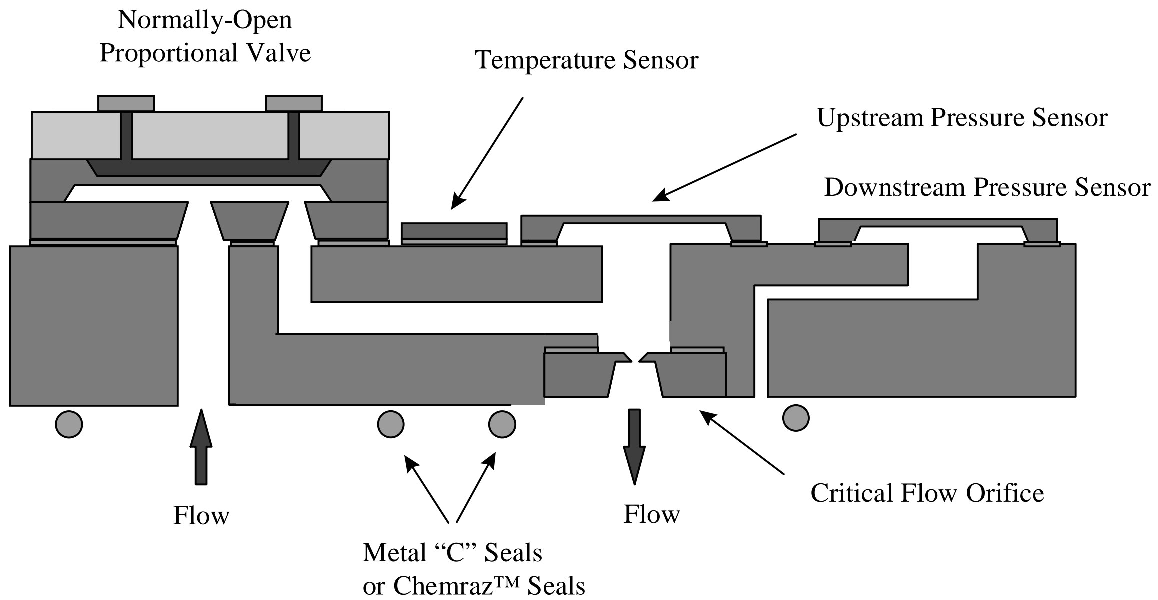

Figure 1. Schematic cross-section of the MEMS-based MFCs used in this study.

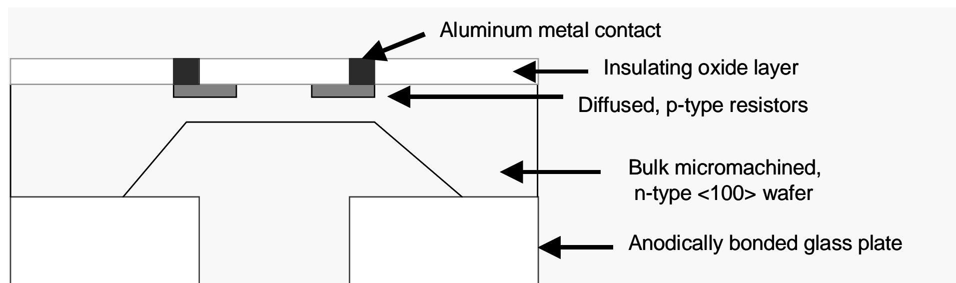

Figure 2a. Schematic cross-sectional view of a piezoresistive pressure sensor.

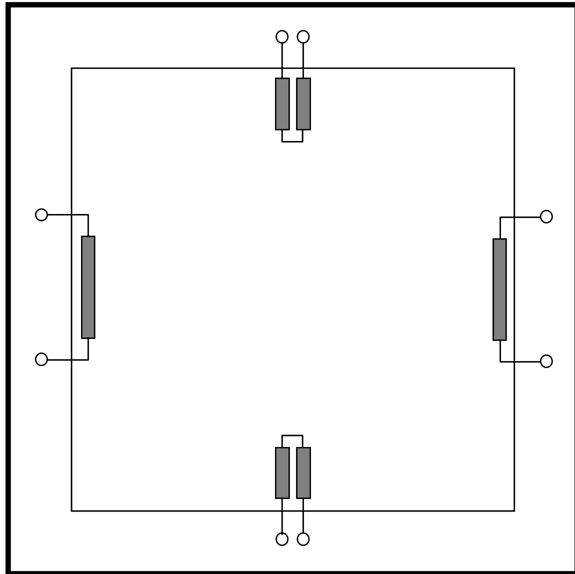

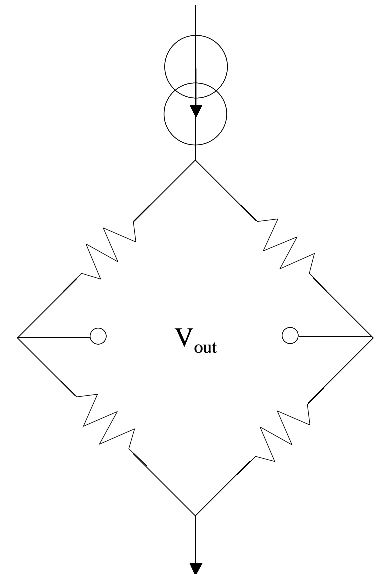

Figure 2b (left). Schematic plan view of a piezoresistive pressure sensor.
Figure 2c (right). Schematic of Wheatstone bridge circuit used in piezoresistive pressure sensors.

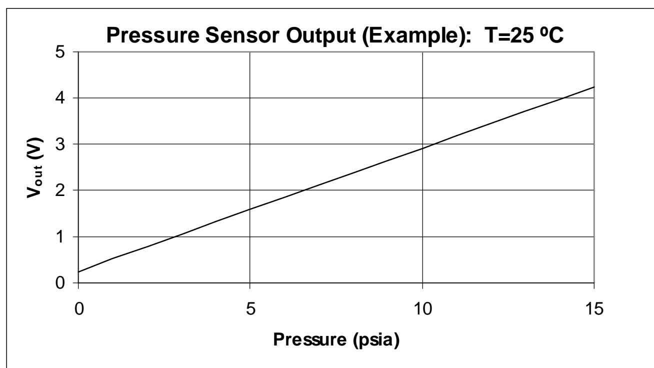

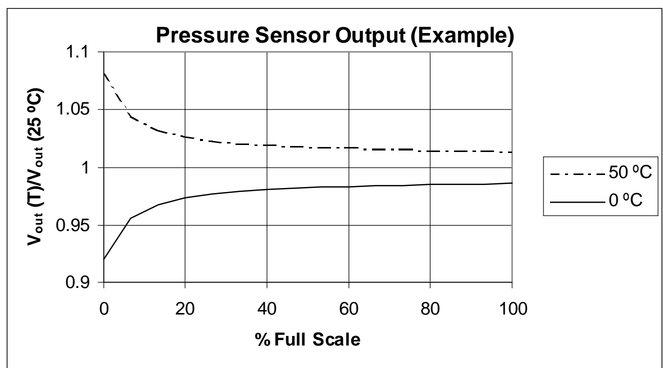

Figure 3a (left). Output voltage vs. excitation pressure for a typical piezoresistive pressure sensor.
Figure 3b (right). Normalized output voltage vs. excitation pressure (as a percent of the full-scale sensor range) and ambient temperature.

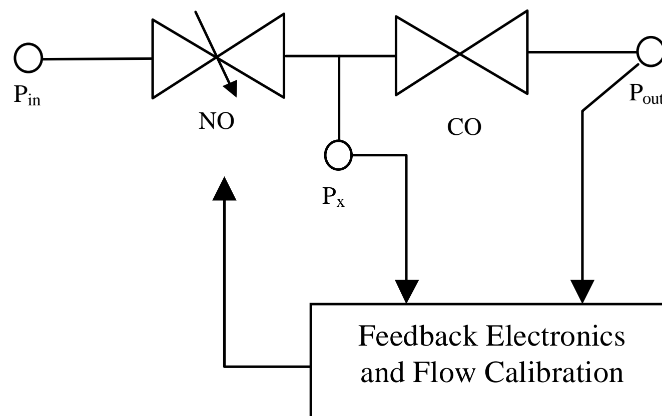

Figure 4. Functional schematic of the MEMS-based MFCs used in this study. 'NO' is the normally-open silicon microvalve. 'CO' is a silicon-microfabricated orifice, typically operating in the sonic flow regime. 'P_x' is the upstream pressure sensor, and 'P_{out}' is the downstream pressure sensor.

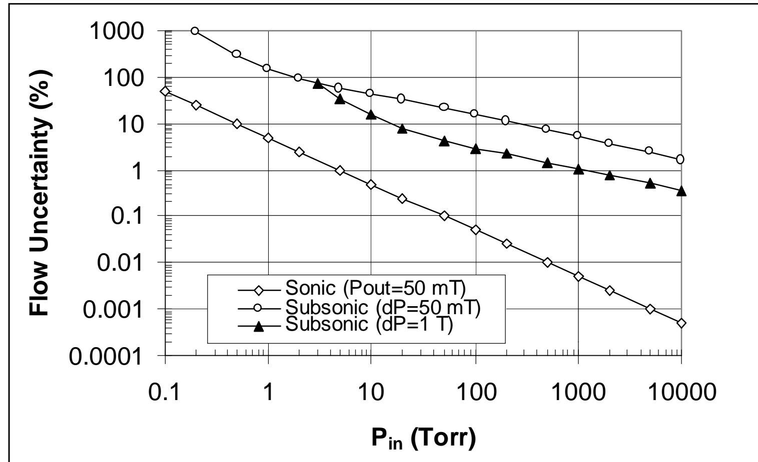

Figure 5. Flow uncertainty vs. flow sensor inlet pressure, for sonic and subsonic flow through the flow sensor orifice. The values of U_P in the uncertainty equation are 50 mT.

3. MFC RELIABILITY CHARACTERIZATION PROCEDURE

Twenty-one mass flow controllers (MFCs) were characterized for reliability in December 2001 and the first half of 2002. Testing occurred at both Redwood Microsystems (RMI), and SMC in Tsukuba, Japan. The MFCs were cycled in the following setpoint sequence: 0-100; 100-25; 25-75; 75-0; repeat. The duration for each of these double-cycles was 5 sec. At specified readouts, each MFC was tested for compliance to the requirements for particle, accuracy, linearity, zero offset, valve leak integrity (leak across valve seat), step response, and inboard leak.

In order to investigate long-term "drift" (technically, long-term reproducibility), a number of other MFCs were tested over periods of up to eighteen months. Performance was monitored on roughly a monthly basis.

Table 1 describes the serial numbers, flow rates, and test location for the MFC devices that were cycle -tested for reliability.

Table 1: Reliability Test Units

Model Number	Serial Number	Full Scale (sccm, N_2)	Test Location
99-0100-1-11-00-1S-N2	1421,1422,1423,1424,1425, 1426,1428,1429,1430,1431	100	SMC
99-0100-1-11-00-1S-N2	1382,1383,1384,1385,1386, 1387,1388	100	RMI
99-0200-1-11-00-2S-N2	1284,1285,1286,1288	200	RMI

Tables 2 and 3 list the tests, standards, and requirements for the cycling reliability characterization[24]. The test procedures are defined in the standards listed. The following are deviations from the reliability standard SEMI E67:

1. SEMI E67, section 7.2 states to perform reproducibility and zero drift as a parametric test. In its place, SEMI E56 was performed, which is a more comprehensive test and includes reproducibility and zero drift.
2. SEMI E67, section 14.6 states to perform all parametric tests on a single MFC before proceeding to the next MFC. This section was not adhered to. In its place, the order of th e parametric tests were adhered to, but testing on MFCs overlapped. This is supported by SEMATECH's version of MFC reliability, SEMASPEC 92071224, which does not specify the test sequence.
3. SEMI E67, Table 1 lists readpoints that are different than the readpoints used in this characterization. SEMI E67, section 3.5 states that different readpoints can be selected.
4. The reliability calculation assumed a 90% confidence and an exponential hazard function. This was used in place of SEMI E67, Appendix 1.

Table 2: Reliability Information. *All tests to be performed at 20-25°C ambient.*

Test	Standard	Additional Requirements
Reliability	SEMI E67 (see notes above)	For Cycling: 20 psig inlet pressure, < 10 torr outlet pressure; Time interval from set point change to the next set point change is 1.25 seconds. One cycle equals 2.5 seconds (refer to Figure 2 in E67).

Table 3: Parametric Tests Information. *All tests to be performed at 20-25°C ambient. Testing may overlap.*

Test Sequence	Parametric Test	Units	Specification	Standard	Additional Requirements
1	Particle (Cycle test)	Particles per cycle	≤ 0.01 particles per cycle larger than 0.02 micron after 120 minute clean up period as measured over 500 cycles	SEMASPEC 92071226-STD	If equipment can not measure <0.1 micron, still perform test and report results
2 (SEMI E56 Test)	Accuracy	%FS	≤ ±1% of the full scale rated flow from 5% to 100% of the rated flow	SEMI E56, SEMASPEC 92071221-STD	Use Molbloc system, DUT: 20 psig inlet pressure, < 10 torr outlet pressure
2 (SEMI E56 Test)	Linearity	%FS	≤ ±1% of the full scale rated flow from 5% to 100% of the rated flow	SEMI E56, SEMASPEC 92071221-STD	Use Molbloc system, DUT: 20 psig inlet pressure, < 10 torr outlet pressure
2 (SEMI E56 Test)	Zero Offset	mV	≤ ±25 mV	SEMI E56, SEMASPEC 92071221-STD	Use Molbloc system, DUT: 20 psig inlet pressure, < 10 torr outlet pressure
2 (SEMI E56 Test)	Valve Leak Across the Seat	%FS	≤1% of full scale rated flow	SEMI E56, SEMASPEC 92071221-STD	Use Molbloc system, DUT: 20 psig inlet pressure, < 10 torr outlet pressure
3	Response	seconds	≤1.25 seconds (step response) ≤ 1.25 seconds (settling time) (spec based on cycling interval)	SEMI E17	Use Honeywell flow sensor, minimum length between Honeywell and DUT connections. 25 psig inlet pressure as stated in SEMI E17, < 10 torr outlet pressure
4	Inboard Leak		$\leq 1 \times 10^{-9}$ atm cc/sec He	SEMI E16	

4. MFC CHARACTERIZATION RESULTS

Figure 6 shows qualitatively[25] the areas of reliability concern, and long-term 'drift' concern. The long-term reproducibility and reliability cycling tests were designed to examine these concerns.

Following the cycling tests, two "soft" failures were observed in the units tested at RMI. One failure was for not-closing, and one was an inboard leak at the C-seals. These "soft" failures will be considered elsewhere[26]. The accuracy results are shown in Figure 7a, while the through-the-valve leak results are shown in Figure 7b. Five of the units tested at SMC (Tsukuba, Japan) exceeded the through-the-valve leak specification (two at 1M cycles, three at the 2M cycle point). All of the units passed the accuracy criteria, although clear evidence of sensor drift was evident.

The long-term reproducibility results are shown in Figure 8. Again, some long-term drift in these units can be discerned, although the overall result is excellent. This figure includes data for units simply held on the shelf, as well as actively cycled.

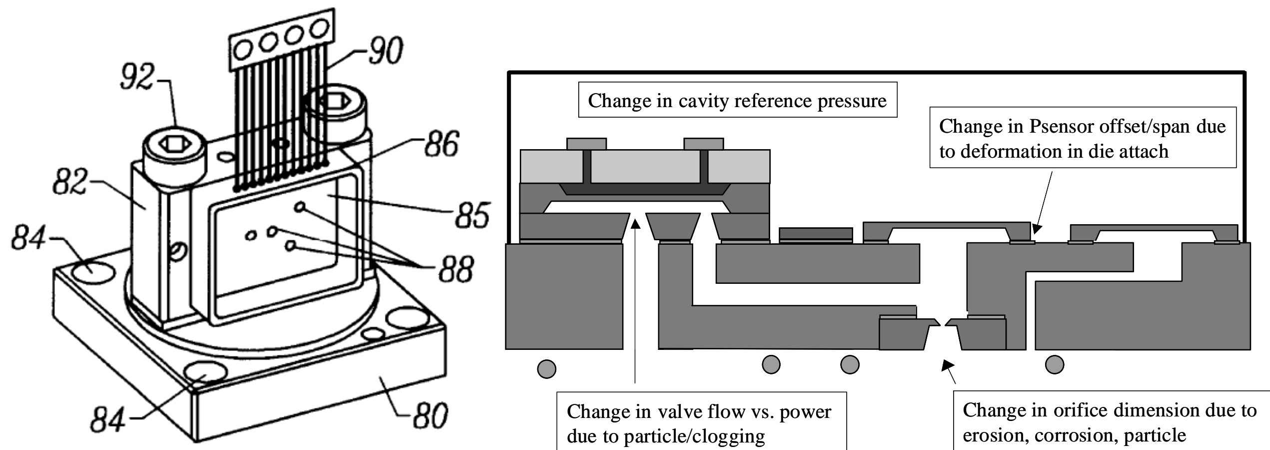

Figure 6. Areas of possible reliability concern for pressure-based MFCs.

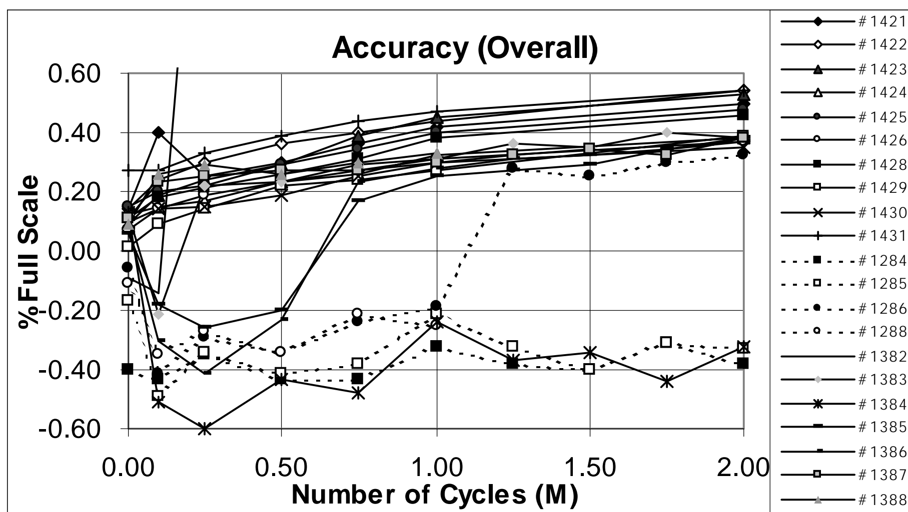

Figure 7a. Accuracy vs. cycling for setpoints from 5% to 100% of full scale (specification: < 1% FS).

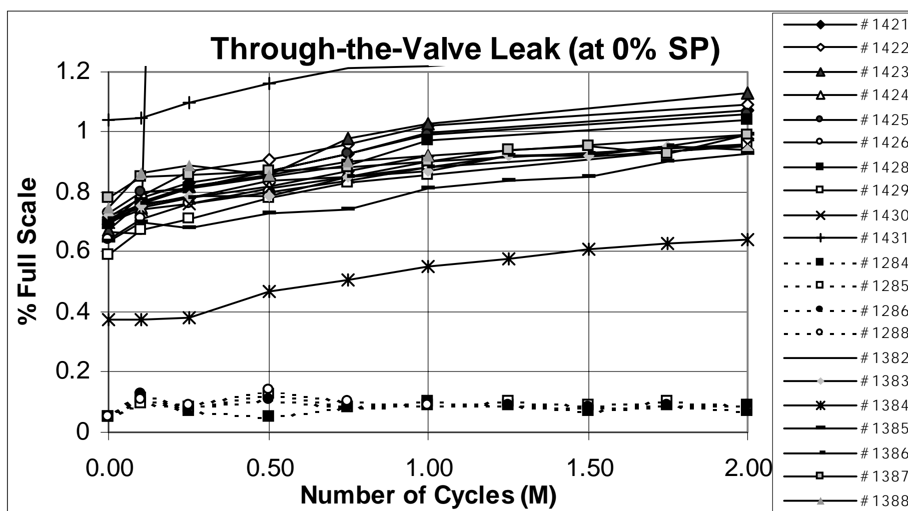

Figure 7b. Through-the-valve leak rate for 0% setpoint command (specification: <1% FS).

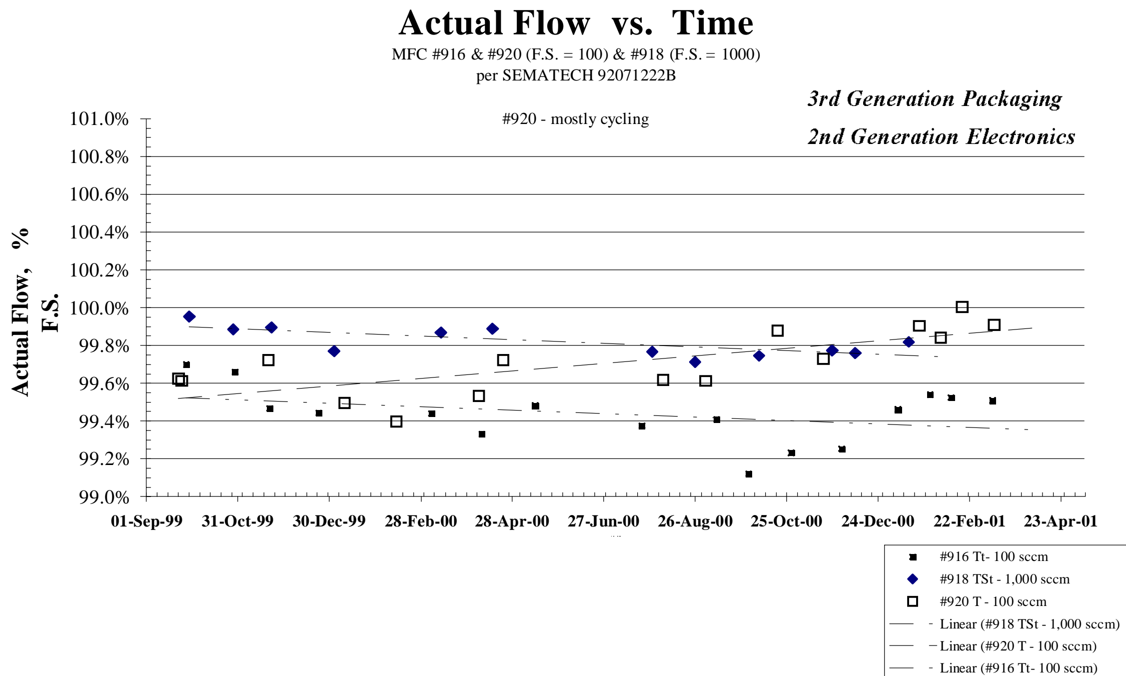

Figure 8. Long-term reproducibility ("drift") time for several pressure-based MFCs.

5. DISCUSSION

The change in accuracy as a function of number of cycles is directly attributable to the behavior of the piezoresistive pressure sensors. As cycling time progresses, relaxation occurs in the pressure sensor die attach material (an epoxy-like material), causing the initial (although minimal) stress in the sensor membrane to dissipate. This initial stress is caused by the difference in thermal expansion coefficient between the package and the silicon die, and the temperature difference between the die attach temperature and the temperature of operation of the MFC. The abrupt change from a negative value of accuracy, to a positive value, is suggestive of an 'oil-canning' effect in the membrane zero-pressure stress characteristic.

Other potential mechanisms for drift are ruled out. *Mechanical* stress on the pressure sensors, due to torques generated by the package hold-down bolts, and the C-seal force, were eliminated several years ago by using the packaging technique shown in Figure 6, wherein the bolt force is perpendicular to the die attach force between the pressure sensors and the package[25]. *Fluidic* changes, as manifested by changes in the silicon orifice dimensions, have never been observed in our devices, for any gas other than the highly corrosive ClF_3. *Electronic* changes, in the form of changes in the stored calibration coefficients (due to, for instance, soft errors in the EPROM memory in which the coefficients are stored) have also never been observed. These coefficients can be read out from memory, and compared to the originally-stored coefficients. Such comparison shows no change. *Pneumatic* changes, due to an increase in the cavity reference pressure above the initial vacuum value, are possible. However, such a change in reference pressure as a function of time has been ruled out. This reference pressure change would cause, at constant temperature, the same sort of accuracy characteristic observed in Figure 7. However, at elevated temperature, the output voltage characteristic of the piezoresistive sensors will <u>increase</u>, indicating a higher pressure (see Figure 3b); while a leak-up in the cavity pressure will cause the output voltage characteristic to <u>decrease</u>.

The conclusion that drift in accuracy vs. cycling is caused by pressure sensor drift is further borne out by the measurements of through-the-valve leak rate for a 0% setpoint. Two of the ten MFCs tested at SMC failed for leak across the seat at 1M cycles (#1422, #1423). Three more failed at 2M cycles (#1421, #1425, #1428). In these units, the flow rate for a 0% setpoint was programmed to be initially equal to 0.5% of full scale, where the flow is derived form the calibration coefficients of the flow sensor. Drift in the pressure sensors, however, caused this 0% setpoint flow to increase, as time and

the number of cycles progressed. To correct the problem, a change was made in the 0% setpoint algorithm. Instead of relying on the flow sensor output, the microvalve power was directly controlled, to be equal to the power required to shut the pre-cycling 0% setpoint flow to less than 0.5% of full scale. Four reliability units tested at RMI were built with this software change (#1284, #1285, #1286, and #1288 – dashed lines in Figures 7). As the data shows for these four units, the valve leak values do not increase as a function of the number of cycles. [Note: #1431 showed failure for leak across the seat at 0 cycles. This should be considered an operator error, not a reliability failure. It had been manufactured with the wrong valve parameters.]

6. CONCLUSIONS

We have carried out an extensive, long-term study of reliability in pressure-based MFCs, with substantial and crucial use of MEMS components, in the flow sensor, and in the microvalve which controls the flow. Studies of MFC accuracy and through-the-valve leak rate at 0% setpoint, indicate that drift in the pressure sensors, which are key to the pressure-based flow sensor, are responsible for the observed changes in accuracy and through-the-valve leak rate. These drift changes are further shown to be caused by thermo-mechanical mechanisms, which relax the stress in the piezoresistive pressure sensor membranes or diaphragms, as the die attach material holding the sensor die to the package alter their mechanical state over time. This time-dependent change in the die attach material is driven by thermal coefficient of expansion differences between the sensor silicon, and the package metal.

The use of novel packaging technology[25], and careful attention to calibration of the pressure sensors as a function of both pressure and package temperature[27], goes far toward the goal of a 'perfect' flow sensor. MFCs built using this unique technology have superior accuracy over their dynamic range, compared to virtually any competing technology. However, extensions of the dynamic range are still desired. To achieve a goal of 0.25% of reading accuracy over a 100:1 dynamic range, with minimal drift over cycling and time, will require one or more of the following: higher-resolution pressure sensor[28]; improvement in the temperature coefficient of expansion match between sensor die and package; and improvement in the thermomechanical relaxation of the sensor die attach material.

7. ACKNOWLEDGEMENTS

Our collaborations with Jim Harris, Mike Selser, John Hill, Hubert Dinh, Jing Chen, and Brad Cozad are acknowledged with gratitude. Redwood Microsystems' collaboration with SMC-Japan's Research and Development team in Tsukuba, Japan, and particularly with Kenji Shinozaki and Toru Horiuchi with respect to this work, is also acknowledged with gratitude.

8. REFERENCES

1. P. W. Barth, "Silicon microvalves for gas flow control." In Proceedings, *Transducers '95 (1995 Int'l. Conf. Sol. State Sens. and Act.)*, pp. 276-279, IEEE, Piscataway, NJ, 1995.
2. M. J. Zdeblick and J. B. Angell, "A microminiature electric-to-fluidic valve." In Proceedings, *Transducers '87 (1987 Int'l. Conf. Sol. State Sens. and Act.)*, pp. 827-830, IEEE, Piscataway, NJ, 1987.
3. K. Engelsdorf and M. Mettner, "Microvalve." US Patent 5,161,774 (1992).
4. H. Jerman, "Electrically-activated, micromachined diaphragm valves." In *Tech. Dig. IEEE Solid-State Sensor and Actuator Workshop*, pp. 65-69, IEEE Press, Piscataway, NJ, 1990.
5. A. D. Johnson and C. A. Ray, "Shape memory film actuated microvalve." US Patent 5,325,880 (1993).
6. T. Ohnstein, T. Fukiura, J. Ridley, and U. Bonne, "Micromachined silicon microvalve." In Proceedings, *IEEE MEMS Workshop*, pp. 95-98, IEEE Press, Piscataway, NJ, 1990.
7. R. G. Johnson, R. E. Higashi, P. J. Bohrer, and R. W. Gehman, "Design and packaging of a highly sensitive microtransducer for air flow and differential pressure sensing applications." In *Proc. 1985 Intl. Conf. Sol.-St. Sens. and Act.*, pp. 358-360 (1985).
8. E. Yoon and K. D. Wise, "A dielectrically-supported multi-element mass flow sensor." In *IEEE IEDM Tech. Dig.*, pp. 670-673 (1988).
9. G. Stemme, "A CMOS integrated silicon gas-flow sensor with pulse modulated output." *Sensors and Actuators* **14**, pp. 293-303 (1988).

10. H.-Y. Hsieh, "Pyroelectric anemometers." Ph.D. dissertation, University of Pennsylvania (1993).
11. A. K. Henning, J. S. Fitch, J. M. Harris, E. B. Dehan, B. A. Cozad, L. Christel, Y. Fathi, D. A. Hopkins, Jr., L. J. Lilly, W. McCulley, W. A. Weber, and M. Zdeblick, "Microfluidic MEMS for semiconductor processing." *IEEE Transactions on Components, Packaging, and Manufacturing Technology* **B21**, pp. 329-337 (1998).
12. J. S. Fitch, A. K. Henning, E. B. Arkilic, J. M. Harris, "Pressure-based mass-flow control using thermopneumatically-actuated microvalves." In *Proceedings, Solid-State Sensor and Actuator Workshop*, pp. 162-165 (Transducers Research Foundation, Cleveland, OH, 1998).
13. A. K. Henning, J. Fitch, J. M. Harris, E. B. Arkilic, B. Cozad, and B. Dehan, "MEMS-based gas distribution and control systems for semiconductor processing." In *Proceedings, Micromachined Devices and Components* (International Society for Optical Engineering, Bellingham, WA, 1998; P. J. French and K. Chau, eds.), volume 3514, pp. 159-170.
14. A. K. Henning, B. A. Cozad, E. Lawrence, E. B. Arkilic, and J. M. Harris, "Practical aspects of micromachined gas distribution systems for semiconductor processing." In Proceedings*, Microfluidic Devices and Systems* (International Society for Optical Engineering, Bellingham, WA, 2000; C. H. Mastrangelo and H. Becker, eds.), vol. 4177, pp. 251-262.
15. M. Esashi, S. Eoh, T. Matsuo, and S. Choi, "The fabrication of integrated mass flow controllers." In Proceedings, *Transducers '87 (1987 Int'l. Conf. Sol. State Sens. and Act.)*, pp. 830-833, Inst. Elec. Eng. Japan, 1987.
16. S. T. Cho and K. D. Wise, "A high-performance microflowmeter with built-in self test." *Sensors and Actuators* **A36**, pp. 47-56, 1993.
17. M. Zdeblick, "Integrated, microminiature electric-to-fluidic valve and pressure/flow regulator." U.S. Patents 4,821,997, 4,824,073, and 4,943,032 (1989).
18. J. Bryzek, "Modeling performance of piezoresistive pressure sensors." In *Proc. 3rd Int. Conf. on Sol.-St. Sens. and Act.*, pp. 168-173 (1985).
19. Y. S. Lee and K. D. Wise, "A batch-fabricated silicon capacitive pressure transducer." *IEEE Trans. Elec. Dev.* **29**, pp. 42-47 (1982).
20. O. N. Tufte, P. W. Chapman, and D. Long, "Silicon diffused-element piezoresistive diaphragms." *J. Appl. Phys.* **33**, p. 3322 (1962).
21. Samaun, K. D. Wise and J. B. Angell, "An IC Piezoresistive Pressure Sensor for Biomedical Instrumentation," *IEEE Trans. Biomed. Engg.*, **BME-20**(2), pp. 101-109 (1973).
22. A. C. M. Gieles and G. H. J. Somers, "Miniature pressure transducers with silicon diaphragm." *Phillips Tech. Rev.* **33**, p. 14 (1973).
23. A. K. Henning, "A compact, pressure- and structure-based gas flow model for microvalves." In *Proceedings, Materials and Device Characterization in Micromachining* (International Society for Optical Engineering, Bellingham, WA, 2000; Y. Vladimirsky and P. J. Coane, eds.), volume 4175.
24. For Tables 2 and 3, see the standards' specifications published and maintained by the Semiconductor Equipment and Materials International (6034 West Courtyard Drive, Suite 315, Austin, TX 78730); and by International SEMATECH (2706 Montopolis Drive, Austin, TX, 78741).
25. M. Selser, E. B. Arkilic, B. A. Taheri, "Apparatus and method for mounting micromechanical fluid control components." U.S. Patent 6,123,107 (2000).
26. E. Lawrence and A. K. Henning, "Reliability of MEMS-based mass-flow controllers for semiconductor processing." In Proceedings, *2003 IEEE Intl. Rel. Phys. Symp.* To be published (2003).
27. J. M. Harris, B. A. Taheri, E. B. Arkilic, "Apparatus and method for correcting drift in a sensor." U.S. Patent 6,237,394 (2001).
28. A. K. Henning, A. Zias, N. Mourlas, and S. Metz, "A MEMS-based, high-sensitivity pressure sensor for ultraclean semiconductor applications." In *Proceedings, 13th IEEE/SEMI Advanced Semiconductor Manufacturing Conference and Workshop (ASMC)* (IEEE, Piscataway, NJ, 2002), pp. 165-168.